Journal of Engineering Mathematics **26**: 481–492, 1992.

Slip at a uniformly porous boundary: effect on fluid flow and mass transfer

SHANKARARAMAN CHELLAM[1], MARK R. WIESNER[1,*] and CLINT DAWSON[2]

*Departments of [1]Environmental Science and Engineering; [2]Mathematical Sciences; Rice University, P.O. Box 1892, Houston, TX 77251, USA (*author for correspondence)*

Received 21 June 1991; accepted in revised form 25 February 1992

Abstract. An approximate solution to the 2-D Navier–Stokes equations for steady, isothermal, incompressible, laminar flow in a channel bounded by one porous wall subject to uniform suction is derived. The solution is valid for small values of the Reynolds number based on the suction velocity and channel height. Solute transport is considered numerically by decoupling the equations representing momentum and mass transfer. The effect of fluid slip at the porous boundary on the axial and transverse components of fluid velocity, axial pressure drop and mass transfer is investigated.

1. Introduction

Crossflow (or tangential flow) membrane filtration has become an important solid-liquid separation process in water treatment in the last two decades. This technique involves the application of a pressure differential to a feed stream flowing tangentially over a porous membrane. While clean solvent (with components smaller than the pores) flows through the membrane, the larger components are removed at the membrane surface and form a layer which in time presents additional resistance to the flow of solvent across the membrane. This phenomenon is termed concentration polarization. Parallel plate membrane modules consisting of a channel bounded by two porous walls are widely used for filtration. Berman [1] first derived approximate expressions for the fluid velocity components for flow in such a module assuming a sufficiently small Reynolds number, Re_w (based on the wall permeation velocity and channel height) and no-slip at both walls. Robinson [2] proved the existence of multiple solutions to the Navier–Stokes equations for $\mathrm{Re}_w > 12.165$. Beavers and Joseph [3] reported mass efflux experiments and proved the existence of a non-zero tangential (slip) velocity on the surface of a permeable boundary. Saffman [4] using a statistical approach, derived a form for the slip velocity u_{slip}, as being proportional to the shear rate:

$$u_{\mathrm{slip}} = -\frac{\sqrt{k}}{\alpha}\frac{\partial u}{\partial y} + O(k)\,, \tag{1.1}$$

where α is a dimensionless constant which depends on the pore size of the permeable material (Beavers and Joseph correlated their experimental data with $\alpha = 0.1$), k is the permeability and y is the inward normal to the porous surface. Singh and Laurence investigated the fluid mechanics and mass transfer in parallel plate and tubular membrane filtration systems assuming equally porous boundaries [5, 6]. In their mass transfer studies, they used extremely high values for the slip coefficient (0.1 and 0.5), which cannot be realized with available membranes. Frequently, laboratory scale parallel plate filters are asymmetric, having only one porous wall, the other wall being solid. Such a geometry is

convenient for conducting experiments; for permeate collection, membrane replacement and concentration measurement. Membrane filtration to separate plasma and cellular components from whole blood (plasmapheresis), is often carried out in a filtration cell with one porous wall, both in laboratory and commercial scale [7]. Experimental mass transfer results obtained from such a filter geometry can be used to gain understanding of flux reduction and polarization phenomena in other membrane filtration geometries. For the mathematical modeling of such experimental data, expressions for the velocity and pressure fields are necessary.

This paper presents a regular perturbation solution describing the flow characteristics in an asymmetric channel with a finite fluid slip velocity at the porous boundary. The steady-state convection-diffusion equation is solved numerically by decoupling the velocity and concentration fields. The effect of fluid slip on the velocity profiles, on the pressure drop and on the mass transfer of Brownian components is also reported. While fluid slip is negligible at a free membrane surface it is proposed to be a useful concept in describing deposition onto a concentration polarization layer and in modeling transport phenomena in dynamic membranes.

2. Formulation of the fluid flow problem

Consider the flow of an incompressible fluid in a channel with one porous wall without the action of external forces. The coordinate system used is given in Fig. 1. L and h denote the length and height of the channel respectively. x is the axial distance coordinate measured from the channel entrance and λ is the dimensionless coordinate in the normal direction ($\equiv y/h$). If the width of the channel is very large compared to the height, the flow can be modeled as being two dimensional. The Navier–Stokes equations of motion describing the transfer of momentum in this case assuming steady, isothermal, laminar flow are

$$u\frac{\partial u}{\partial x}+\frac{v}{h}\frac{\partial u}{\partial \lambda}=-\frac{1}{\rho}\frac{\partial P}{\partial x}+\nu\left(\frac{\partial^2 u}{\partial x^2}+\frac{1}{h^2}\frac{\partial^2 u}{\partial \lambda^2}\right), \tag{2.1}$$

$$u\frac{\partial v}{\partial x}+\frac{v}{h}\frac{\partial v}{\partial \lambda}=-\frac{1}{\rho h}\frac{\partial P}{\partial \lambda}+\nu\left(\frac{\partial^2 v}{\partial x^2}+\frac{1}{h^2}\frac{\partial^2 v}{\partial \lambda^2}\right), \tag{2.2}$$

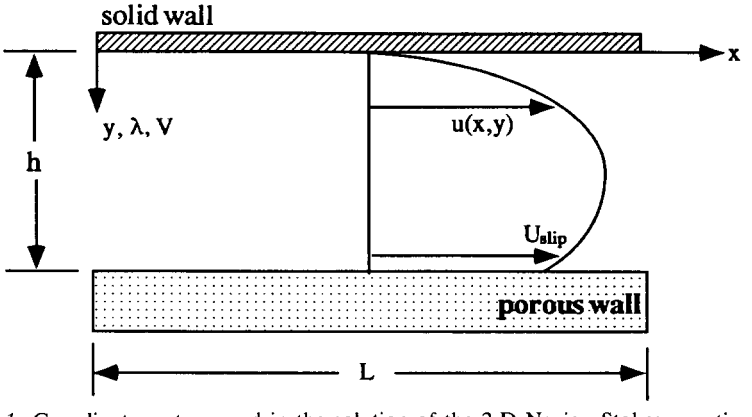

Fig. 1. Coordinate system used in the solution of the 2-D Navier–Stokes equations.

where P and ν denote the fluid pressure and kinematic viscosity respectively and u and v are the velocity components in the axial and transverse directions. The continuity equation representing a conservation of mass for this fluid is written as

$$\frac{\partial u}{\partial x} + \frac{1}{h}\frac{\partial v}{\partial \lambda} = 0 . \tag{2.3}$$

The boundary conditions are

$$u = 0 \quad \text{at } \lambda = 0 , \tag{2.4}$$

$$v = 0 \quad \text{at } \lambda = 0 , \tag{2.5}$$

$$v = v_w \quad \text{at } \lambda = 1 , \tag{2.6}$$

$$u = u_{\text{slip}} = -\frac{\sqrt{k}}{\alpha h}\frac{\partial u}{\partial \lambda} \quad \text{at } \lambda = 1 . \tag{2.7}$$

Equations (2.4) and (2.5) are the no-slip boundary conditions for a viscous fluid at the surface of the solid wall. Equation (2.6) denotes that the suction rate at the permeable wall, v_w is constant along the length of the channel. Equation (2.7) is derived from Eq. (1.1) assuming that the term $O(k)$ can be neglected compared to the term $O(\sqrt{k})$ (valid for $k \ll 1$). This boundary condition allows for a tangential component of fluid velocity along the porous boundary.

3. Perturbation solution of the equations of motion

The solution technique followed here was first formulated by Berman [1]. For incompressible flows, the velocity vector $\mathbf{v}$ can be expressed in terms of a vector potential $\boldsymbol{\psi}$ as

$$\mathbf{v} = \nabla \times \boldsymbol{\psi} . \tag{3.1}$$

In two dimensions, in terms of the scalar stream function ψ, we write

$$u = \frac{\partial \psi}{\partial y} = \frac{1}{h}\frac{\partial \psi}{\partial \lambda} , \tag{3.2}$$

$$v = -\frac{\partial \psi}{\partial x} . \tag{3.3}$$

Let u_0 represent the uniform inlet velocity. We introduce a stream function from a mass balance on the fluid in the channel as

$$\psi = [hu_0 - v_w x] f(\lambda) , \tag{3.4}$$

where $f(\lambda)$ is an unknown function of the distance coordinate λ. Substituting Eq. (3.4) into Eqs (3.2) and (3.3) expressions are obtained for the velocity components as

$$u = (u_0 - v_w x/h) f'(\lambda) , \tag{3.5}$$

$$v = v_w f(\lambda) . \tag{3.6}$$

When Eqs (3.5) and (3.6) are substituted into Eqs (2.1) and (2.2) we obtain

$$\left(u_0 - \frac{v_w x}{h}\right)\left\{-\frac{v_w}{h}\left[(f')^2 - ff''\right] - \frac{\nu}{h^2} f'''\right\} = -\frac{1}{\rho}\frac{\partial P}{\partial x} , \tag{3.7}$$

$$\frac{v_w^2}{h} ff' - \frac{\nu v_w}{h^2} f'' = -\frac{1}{\rho h}\frac{\partial P}{\partial \lambda} . \tag{3.8}$$

We note that the left hand side of Eq. (3.8) is a function of λ only (i.e. independent of x). Assuming the pressure is twice differentiable we can differentiate Eq. (3.8) w.r.t. x to get

$$\frac{\partial^2 P}{\partial x\, \partial \lambda} = 0 , \quad \text{or} \quad \frac{\partial^2 P}{\partial \lambda\, \partial x} = 0 . \tag{3.9}$$

Differentiating Eq. (3.7) with respect to λ and simplifying we obtain

$$\frac{\partial}{\partial \lambda}\left\{\frac{v_w}{h}\left[(f')^2 - ff''\right] + \frac{\nu}{h^2} f'''\right\} = 0 . \tag{3.10}$$

Integrate Eq. (3.10) and simplify to get the ordinary differential equation

$$\mathrm{Re}_w\left[(f')^2 - ff''\right] + f''' = C , \tag{3.11}$$

where Re_w is a wall Reynolds number ($\equiv v_w h/\nu$) and C is the constant of integration. An approximate perturbation solution to Eq. (3.11) is possible if we treat Re_w as the perturbation parameter, i.e. Re_w must be sufficiently small. We look for a solution of the form

$$f(\lambda) = f_0(\lambda) + \mathrm{Re}_w f_1(\lambda) + \mathrm{Re}_w^2 f_2(\lambda) + \cdots + \mathrm{Re}_w^n f_n(\lambda) + \cdots , \tag{3.12}$$

$$C = C_0 + \mathrm{Re}_w C_1 + \mathrm{Re}_w^2 C_2 + \cdots \mathrm{Re}_w^n C_n + \cdots , \tag{3.13}$$

where f_i and C_i are independent of Re_w. Collecting powers of Re_w we get

0th order: $$f_0''' = C_0 , \tag{3.14}$$

1st order: $$f_1''' = C_1 + f_0 f_0'' - (f_0')^2 , \tag{3.15}$$

2nd order: $$f_2''' = C_2 - 2f_0' f_1' + f_0 f_1'' + f_0'' f_1 . \tag{3.16}$$

The boundary conditions (Eqs 2.4–2.7) transform into

$$f_i' = 0 \qquad \text{at } \lambda = 0 \text{ for } i \geq 0 , \tag{3.17}$$

$$f_i = 0 \qquad \text{at } \lambda = 0 \text{ for } i \geq 0 , \tag{3.18}$$

$$f_0 = 1 \quad \text{and} \quad f_i = 0 \quad \text{at } \lambda = 1 \text{ for } i \geq 1 , \tag{3.19}$$

$$f_i' = -\phi f_i'' \qquad \text{at } \lambda = 1 \text{ for } i \geq 0 , \tag{3.20}$$

where ϕ is the slip coefficient ($\equiv \sqrt{k}/\alpha h$). The zeroth order solution obtained by solving Eq. (3.14) along with the boundary conditions given by Eqs (3.17)–(3.20) is

$$f_0 = -\frac{2(1+\phi)}{(1+4\phi)}\lambda^3 + \frac{3(1+2\phi)}{(1+4\phi)}\lambda^2 . \tag{3.21}$$

The first order solution is

$$f_1 = K_1\frac{\lambda^3}{6} + K_2\frac{\lambda^2}{2} - \frac{12(1+\phi)^2}{210(1+4\phi)^2}\lambda^7 + \frac{(1+\phi)(1+2\phi)}{5(1+4\phi)^2}\lambda^6 - \frac{3(1+2\phi)^2}{10(1+4\phi)^2}\lambda^5 , \tag{3.22}$$

where K_1 and K_2 are constants that depend only on the slip coefficient.

$$K_1 = \frac{-1}{(1+4\phi)^3}\left\{\frac{24(1+\phi)^3}{35} - \frac{12(1+\phi)^2(1+2\phi)}{5} + \frac{36(1+\phi)(1+2\phi)^2}{10} - \frac{12(1+\phi)^2(1+6\phi)}{5} + \frac{36(1+\phi)(1+2\phi)(1+5\phi)}{5} - 9(1+4\phi)(1+2\phi)^2\right\}, \tag{3.23}$$

$$K_2 = \frac{1}{(1+4\phi)^3}\left\{\frac{12(1+2\phi)(1+\phi)^2}{35} - \frac{4(1+\phi)^2(1+6\phi)}{5} - \frac{6(1+\phi)(1+2\phi)^2}{5} + \frac{9(1+2\phi)^3}{5} + \frac{12(1+\phi)(1+2\phi)(1+5\phi)}{5} - 3(1+4\phi)(1+2\phi)^2\right\}. \tag{3.24}$$

The velocity profiles can now be written as

$$u(x, \lambda) = (u_0 - v_w x/h)(f_0' + \mathrm{Re}_w f_1') \tag{3.25}$$

and

$$v(\lambda) = v_w(f_0 + \mathrm{Re}_w f_1) . \tag{3.26}$$

Mid-channel axial and transverse velocities normalized by the local maximum values are shown in Figs 2 and 3 for various values of the slip coefficient. Increasing slip is observed to decrease the shear rate at the porous wall and results in flatter axial velocity profiles. When $\phi = 0$ (no-slip), the expressions described here reduce to the one given by Green [8]. An entrance Reynolds number Re_{ent} ($\equiv u_0 h/\nu$) is introduced and hence, dimensionless streamlines Ψ^*, are given by

$$\Psi^*(x, \lambda) = \frac{\psi(x, \lambda)}{hu_0} = \left(1 - \frac{\mathrm{Re}_w}{\mathrm{Re}_{ent}}\frac{x}{h}\right)(f_0(\lambda) + \mathrm{Re}_w f_1(\lambda)) , \tag{3.27}$$

To visualize the flow, non-dimensional streamlines are plotted in Fig. 4. It is observed that the streamlines are not orthogonal to the porous wall resulting in a non-zero normal derivative and therefore a finite value for the slip velocity. The expression for the dimensionless pressure drop ΔP, along the channel length can be derived from Eqs (3.7) and (3.8) as

$$\Delta P = \frac{p(0, \lambda) - p(x, \lambda)}{\frac{1}{2}\rho u_0^2} = -\frac{2C\nu}{h^2 u_0^2}\left(u_0 x - \frac{v_w x^2}{2h}\right) . \tag{3.28}$$

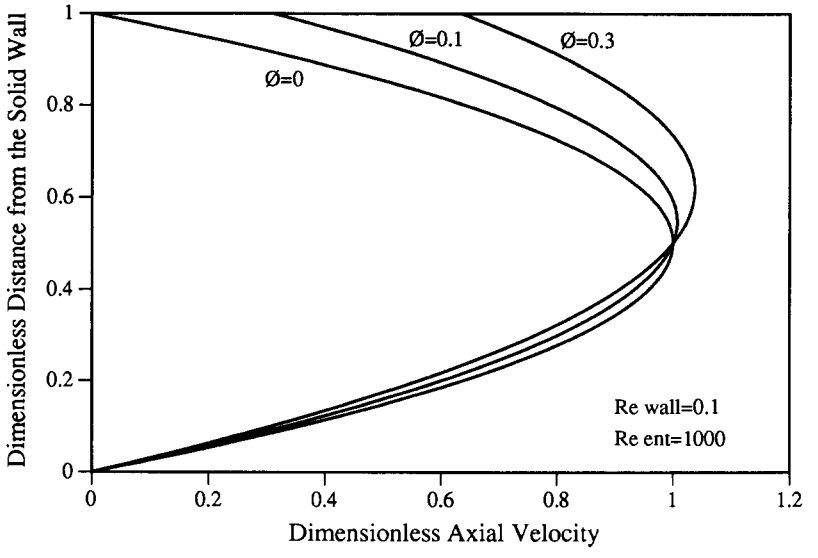

Fig. 2. Effect of the slip coefficient on the mid-channel axial velocity.

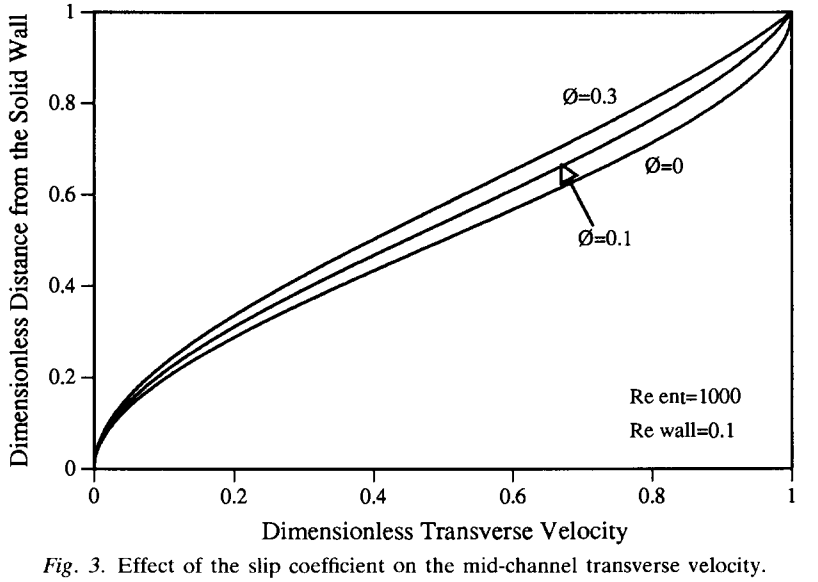

Fig. 3. Effect of the slip coefficient on the mid-channel transverse velocity.

Figure 5 depicts the effect of the slip coefficient on the axial pressure drop; increasing slip is observed to decrease the axial pressure drop.

4. Formulation of the mass transfer problem

In all tangential flow membrane systems, $v_w \ll u_0$. Therefore diffusion in the axial direction can be neglected in comparison to diffusion in the transverse direction. Consider a feed stream having a uniform concentration c_0, across the inlet cross section (Eq. 4.4). The two dimensional convection-diffusion equation describing the transfer of mass at steady state in

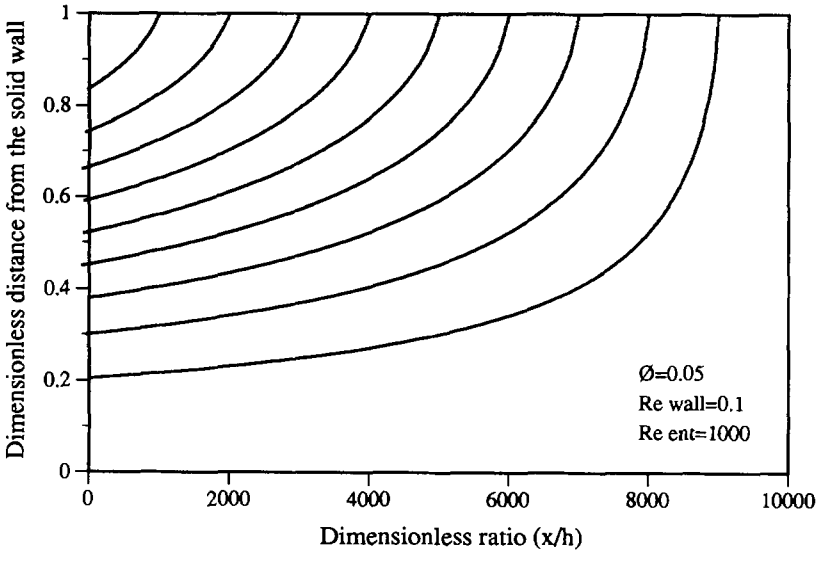

Fig. 4. Dimensionless streamlines for slip flow ($\phi = 0.05$) at the porous wall.

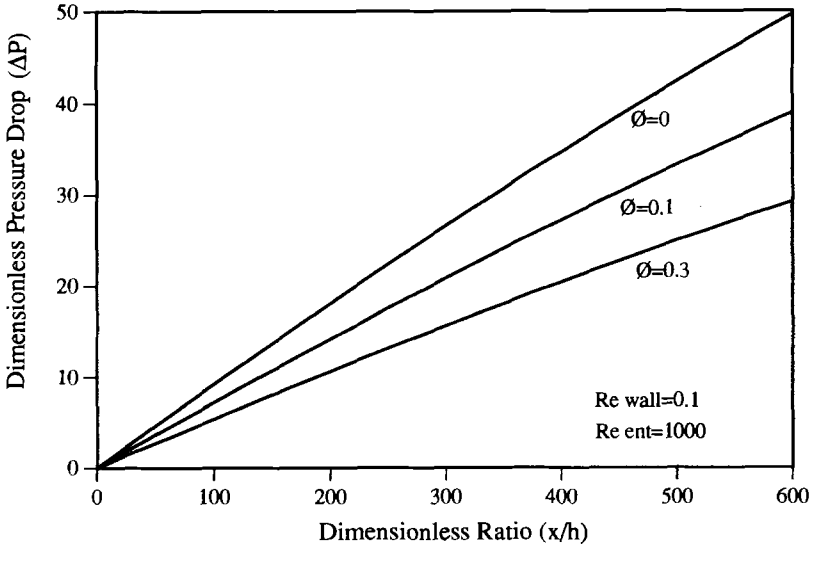

Fig. 5. Variation in the pressure drop in the channel as a function of the slip coefficient.

such a system is

$$u \frac{\partial c}{\partial x} + v \frac{\partial c}{\partial y} = D \frac{\partial^2 c}{\partial y^2}, \tag{4.1}$$

where D is the diffusion coefficient of the solute and c denotes the concentration of the solute. Equation 4.1 along with the boundary conditions given below constitute a complete description of mass transfer in a membrane system.

$$\frac{\partial c}{\partial y} = 0 \qquad \text{at } y = 0, \tag{4.2}$$

$$D\frac{\partial c}{\partial y} = v_w c_w \quad \text{at } y = h\,, \tag{4.3}$$

$$c = c_0 \qquad \text{at } x = 0\,. \tag{4.4}$$

We impose the no-flux boundary condition at the solid wall (Eq. 4.2). Equation (4.3) is the boundary condition for a perfectly rejecting membrane, i.e., no solute passes through the porous interface. Hence, at steady state the convective transport of solute towards the porous wall is balanced by diffusive back transport of material in the side of the fluid continuum. This dynamic exchange of material results in a steady concentration boundary layer thickness. c_w represents the unknown solute concentration at the porous wall.

5. Numerical solution of the mass transfer problem

Introduce the following non-dimensional variables in Eq. 4.1

$$u^* = \frac{u}{u_0}\,, \qquad v^* = \frac{v}{v_w}\,, \qquad c^* = \frac{c}{c_0}\,, \qquad x^* = \frac{x}{L}\,, \qquad \lambda = \frac{y}{h}\,, \tag{5.1}$$

and rearrange to get in dimensionless form

$$u^*\frac{\partial c^*}{\partial x^*} + \left(\frac{v_w L}{u_0 h}\right) v^*\frac{\partial c^*}{\partial \lambda} = \frac{DL}{u_0 h^2}\frac{\partial^2 c^*}{\partial \lambda^2}\,. \tag{5.2}$$

The boundary conditions are also expressed in dimensionless form as

$$c^* = 1 \qquad \text{at } x^* = 0 \text{ for all } \lambda\,, \tag{5.3}$$

$$\frac{\partial c^*}{\partial \lambda} = 0 \qquad \text{at } \lambda = 0 \text{ for all } x^*\,, \tag{5.4}$$

$$\frac{\partial c^*}{\partial \lambda} = v^*\frac{c_w}{c_0}\frac{v_w h}{D} \quad \text{at } \lambda = 1 \text{ for all } x^*\,. \tag{5.5}$$

Let the channel inlet and exit be denoted by $m = 1$ and $m = m_{\max}$ respectively; the solid and porous walls are represented by $j = 1$ and $j = j_{\max}$. Introduce the backward difference approximations for the derivatives in Eq. 4.6 and rearrange to get the finite difference equation

$$A_{j-1}c^*_{j-1m} + B_j c^*_{jm} + E_j c^*_{j+1m} = F_j \quad \text{for } 2 \leq j \leq j_{\max} - 1\,, \tag{5.6}$$

where

$$A_{j-1} = -v^*_j\left(\frac{v_w L}{u_0 h}\right)\frac{1}{\Delta\lambda} - \left(\frac{DL}{u_0 h^2}\right)\frac{1}{(\Delta\lambda)^2}\,, \tag{5.7}$$

$$B_j = \frac{u^*_j}{\Delta x^*} + v^*_j\left(\frac{v_w L}{u_0 h}\right)\frac{1}{\Delta\lambda} + 2\left(\frac{DL}{u_0 h^2}\right)\frac{1}{(\Delta\lambda)^2}\,, \tag{5.8}$$

$$E_j = -\left(\frac{DL}{u_0 h^2}\right) \frac{1}{(\Delta\lambda)^2}\,, \tag{5.9}$$

$$F_j = \frac{u_j^*}{\Delta x^*}\, c_{jm-1}^*\,. \tag{5.10}$$

These coefficients are valid for all the interior points. At the porous and solid boundaries we use the boundary conditions (4.2) and (4.3) and simplify to get the finite difference equation valid at the solid wall

$$B_1 c_{1m}^* + E_1 c_{2m}^* = 0 \quad \text{for } j = 1\,. \tag{5.11}$$

The coefficients B_1 and E_1 are

$$B_1 = v_1^*\left(\frac{v_w L}{u_0 h}\right)\frac{1}{\Delta\lambda} + 2\left(\frac{DL}{u_0 h^2}\right)\frac{1}{(\Delta\lambda)^2}\,, \tag{5.12}$$

$$E_1 = -v_1^*\left(\frac{v_w L}{u_0 h}\right)\frac{1}{\Delta\lambda} - 2\left(\frac{DL}{u_0 h^2}\right)\frac{1}{(\Delta\lambda)^2}\,, \tag{5.13}$$

The finite difference equation at the porous wall can be obtained similarly as

$$A_{j_{\max}-1} c_{j_{\max}-1m}^* + B_{j_{\max}} c_{j_{\max}m}^* = F_{j_{\max}} \quad \text{for } j = j_{\max}\,. \tag{5.14}$$

The coefficients are as given below

$$A_{j_{\max}-1} = -v_{j_{\max}}^*\left(\frac{v_w L}{u_0 h}\right)\frac{1}{\Delta\lambda} - 2\left(\frac{DL}{u_0 h^2}\right)\frac{1}{(\Delta\lambda)^2}\,, \tag{5.15}$$

$$B_{j_{\max}} = \frac{u_{j_{\max}}^*}{\Delta x^*} + v_{j_{\max}}^*\left(\frac{v_w L}{u_0 h}\right)\frac{1}{\Delta\lambda} + 2\left(\frac{DL}{u_0 h^2}\right)\frac{1}{(\Delta\lambda)^2} - 2\,\frac{v_{j_{\max}}^* v_w L}{h u_0\,\Delta\lambda}\,, \tag{5.16}$$

$$F_{j_{\max}} = \frac{u_{j_{\max}}^*}{\Delta x^*}\, c_{j_{\max}m-1}^*\,. \tag{5.17}$$

These coefficients constitute a tridiagonal system of the form

$$\begin{bmatrix} B_1 & E_1 & & & & & & \\ A_1 & B_2 & E_2 & & & & & \\ & A_2 & B_3 & E_3 & & & & \\ & & & A_{i-1} & B_i & E_i & & \\ & & & & A_{j_{\max}-2} & B_{j_{\max}-1} & E_{j_{\max}-1} & \\ & & & & & A_{j_{\max}-1} & B_{j_{\max}} \end{bmatrix} \begin{bmatrix} c_1^* \\ c_2^* \\ \cdot \\ c_{j_{\max}-1}^* \\ c_{j_{\max}}^* \end{bmatrix} = \begin{bmatrix} F_1 \\ F_2 \\ F_3 \\ \vdots \\ F_{j_{\max}-1} \\ F_{j_{\max}} \end{bmatrix} \tag{5.18}$$

Full details of the solution and the computer code for solving the system of linear equations (5.18) are given elsewhere [9]. The effect of slip on solute accumulation near the porous wall is illustrated in Fig. 6. The wall concentration and solute accumulation near the porous boundary is seen to decrease when the slip coefficient is increased. Singh and Laurence [5] in

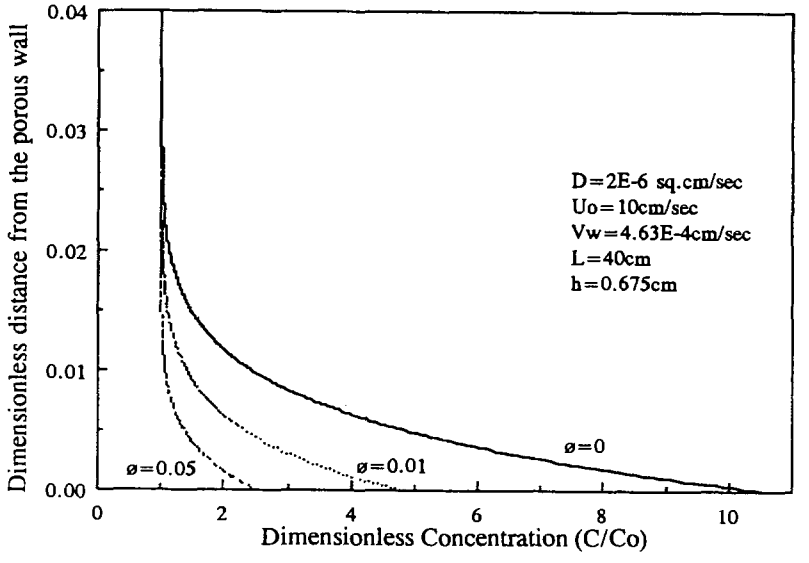

Fig. 6. Effect of fluid slip on concentration profiles near the porous wall at mid-channel.

their investigation on concentration polarization in a parallel plate membrane system with two porous walls had obtained a similar result.

6. Discussion

Most commercial membranes are cast with a constant permeability. The pressure drop along the length of the channel would therefore ensure that the wall permeation rate decreases along the length of the duct. Thus, the assumption of constant wall suction rate is only an approximation even in the initial stages of filtration. Also, in solving the convection-diffusion equation, the field equations representing momentum and mass transfer have been decoupled. Fluid and solute properties such as viscosity, density and diffusivity may change as polarization occurs. The relative importance of viscous and diffusive effects on solute transport is given by the magnitude of the Schmidt number, $Sc(\equiv \nu/D)$. In most membrane filtration applications $Sc \approx O(10^3)$. This indicates that the concentration boundary layer occupies only a small fraction of the channel and that the momentum boundary layer fills the entire channel after a very short entrance region [9]. For example in Fig. 7, $Sc = 5 \times 10^3$ and the maximum thickness of the polarized layer is only 3.5% of the channel height. Only in such instances is a separate treatment of momentum and mass transfer justified. In this case, Eq. 4.1 can be solved using the velocity components given in Eqs 3.25 and 3.26 to generate concentration profiles. Figure 7 shows the concentration boundary layer thickness in a membrane filter as a function of axial distance at various values of the slip coefficient using the same parameters used in generating Fig. 6. The concentration boundary layer is defined here as the region where the solute concentration is at least 1% higher than in the bulk fluid. It is observed that at any particular value of ϕ, the boundary layer thickness increases with increasing axial distance from the channel entrance. Therefore, even if the permeability of a clean membrane were adjusted to give a constant suction velocity, non-uniform polarization of material on the membrane surface at steady state would present non-uniform hydraulic

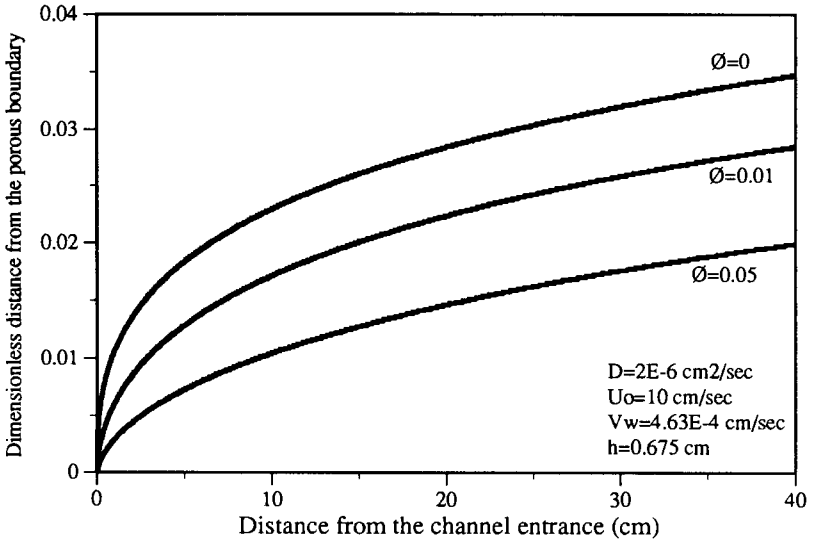

Fig. 7. Growth of concentration boundary layers in the membrane filter at different slip coefficients.

resistance for solvent flow across the permeable boundary. Thus, the suction rate can be expected to decrease along the channel length once a filter is put into operation. Even with these approximations, the model developed for the fluid mechanics has been found to accurately predict convective transport in mass transport experiments conducted in our laboratory [10].

7. Summary and conclusions

The fluid mechanics of a membrane filtration module having one porous wall has been investigated using a regular perturbation technique initially proposed by Berman [1]. Approximate expressions, correct up to $O(\mathrm{Re}_w)$ for the axial and transverse velocities and axial pressure drop incorporating fluid slip at the porous boundary were derived. At steady state, solute accumulation near the porous boundary is determined by a balance between convective and diffusive transport. The analysis presented for mass transfer is valid only for perfectly rejecting membranes and for large values of the Schmidt number. Increasing the magnitude of the slip coefficient was found to decrease the shear rate at the porous wall and also to alleviate concentration polarization.

It is important to note that the slip velocity plays a negligible role at the free membrane surface. $\phi \approx O(10^{-5})$ for membrane permeabilities of $k \approx O(10^{-17})\,\mathrm{m}^2$. However, slip may be used to model fluid mechanics and mass transfer when membranes are coated with a porous deposit. For example, very open structures formed by aggregated colloidal materials deposited on the membrane surface may result in high permeabilities at the surface of the polarized layer. Assuming an aggregate porosity of 95% for a deposit containing 1 μm particles, the permeability is $\approx O(10^{-12})\,\mathrm{m}^2$ corresponding to a slip coefficient of $\phi \approx O(10^{-2})$. Thus, previously deposited material may play an important role in determining subsequent deposition on the concentration-polarization layer. In some filtration applications, materials expected to exhibit filtration properties themselves are intentionally deposited onto porous supports. These secondary layers, termed dynamic membranes are used in

some commercial reverse osmosis units. The concept of fluid slip might therefore be a useful tool for modeling the fluid mechanics and mass transfer in such dynamic membrane systems.

Acknowledgements

Support for this work was provided by the National Science foundation (Grant No. BCS-8909722). Any opinions, findings and conclusions or recommendations expressed in this publication are those of the authors and do not necessarily reflect the views of the National Science foundation.

References

1. A.S. Berman, Laminar flow in channels with porous walls. *Journal of Applied Physics* 24 (1953) 1232–1235.
2. W.A. Robinson, The existence of multiple solutions for the laminar flow in a uniformly porous channel with suction at both walls. *Journal of Engineering Mathematics* 10 (1976) 23–40.
3. G.S. Beavers and D.D. Joseph, Boundary conditions at a naturally permeable wall. *Journal of Fluid Mechanics* 30 (1967) 197–207.
4. P.G. Saffman, On the boundary condition at the surface of a porous medium. *Studies in Applied Mathematics* 50 (1971) 93–101.
5. R. Singh and R.L. Laurence, Influence of slip velocity at a membrane surface on ultrafiltration performance – I. Channel flow system. *International Journal of Heat and Mass Transfer* 22 (1979) 721–729.
6. R. Singh and R.L. Laurence, Influence of slip velocity at a membrane surface on ultrafiltration performance – II. Tube flow system. *International Journal of Heat and Mass Transfer* 22 (1979) 731–737.
7. F. Castino, L.I. Friedman, B.A. Solomon, C.K. Colton and M.J. Lysaght, The filtration of plasma from whole blood: A novel approach to clinical detoxification. In: T.M.S. Chang (ed.), *Artificial Kidney, Artificial Liver and Artificial Cells*. New York: Plenum Press (1978) pp. 259–266.
8. G.A. Green, Laminar flow through a channel with one porous wall, Course project in advanced fluid mechanics. (1979) Department of Chemical and Environmental Engineering, RPI, Troy, NY, USA.
9. S. Chellam, Fluid mechanics and particle transport in a channel with one porous wall: Application to membrane filtration. (1991) Masters thesis, Department of Environmental Science and Engineering, Rice University, Houston, TX, USA.
10. S. Chellam and M.R. Wiesner, Particle transport in clean membrane filters in laminar flow. *Environmental Science and Technology* (1992). In Press.